

## THE REAR INFLOW JET IN MESOSCALE CONVECTIVE SYSTEMS

Bradley F. Smull and Robert A. Houze, Jr.

Department of Atmospheric Sciences, AK-40  
University of Washington  
Seattle, WA 98195

### 1. Introduction

Through analysis of Doppler radar data for a squall-line system that passed over Oklahoma on 22 May 1976, Smull and Houze (1985, 1986) have shown that in its mature stage the storm contained a mesoscale maximum of front-to-rear, system-relative airflow at midlevels. This feature was instrumental in the transport of ice particles originating along a leading line of intense convective cells rearward into a trailing region of stratiform precipitation. Near the precipitation echo's back edge, the front-to-rear flow was opposed by another strong midlevel current, which approached the system from the rear. As it breached the back edge of the system, this "rear inflow jet" eroded the stratiform echo and produced a concavity that Smull and Houze (1985) termed the "rear echo notch." A shortcoming of the 22 May 1976 data set was that the bulk of the rear inflow jet, and thus its interaction with the opposing front-to-rear flow, lay outside the region of Doppler radar coverage. Special network rawinsonde data (not presented here) for times after the period of Doppler analysis indicate that the rear inflow jet eventually penetrated well into the stratiform region, whereupon it approached the leading convective line and greatly accelerated its forward motion. This forward bowing of the squall line immediately preceded the rapid demise of its constituent convective cells. Thus, the rear inflow jet may have ultimately led to the storm's dissipation.

In this paper, we focus on single-Doppler radar data from the 1985 Oklahoma-Kansas PRE-STORM experiment (Houze and Rutledge, 1986). During that experiment, several mesoscale convective systems with rear inflow jets were extensively documented. Here we present examples of the jets in two cases that were observed over Kansas, on 11 June and 28 May 1985. Analyzed data are displayed in vertical (range-height) cross sections along selected azimuths extending from the NCAR CP-4 C-band radar, which was located at Cheney State Park, Kansas ( $\approx 30$  km west-northwest of Wichita).

### 2. Vertical cross sections

Figures 1 and 2 present cross sections reconstructed from volume scans ( $360^\circ$  tilt-sequences) conducted from 0345-0353 GMT on 11 June and 1301-1313 GMT on 28 May, respectively. Analyses of radar reflectivity [ $\text{dB}(Z)$ ] and system-relative horizontal velocity (m/s) are shown. The system-relative horizontal velocities ( $V_h$ ) have been derived from the observed mean radial velocities ( $V_r$ ) using the relation

$$V_h = V_r \cos \alpha + V_t \sin \alpha - V_s$$

where  $\alpha$  is the elevation angle,  $V_t$  is the terminal fallspeed (positive downward), and  $V_s$  is the component of system motion along the direction of the cross section (positive away from the radar). For consistency,  $V_r$  and  $V_h$  are also taken positive away from the radar. (Arrows have been employed in the figures to avoid confusion.)  $V_t$  was estimated from reflectivity data using separate relations for solid and liquid precipitation following Marks and Houze (1986). Since this technique is quite sensitive to errors in the assumed fallspeed at large elevation angles, analysis was limited to regions where  $\alpha < 20^\circ$ . Also, data points were shifted in range to correct for the effects of system translation during the time interval required to complete a volume scan ( $\approx 10$  min); the magnitude of this correction approached 5 km for the highest elevation angles.

Figure 1 depicts reflectivity and velocity patterns for two cross sections separated by  $180^\circ$  in azimuth ( $310^\circ$  and  $130^\circ$ ) through the 11 June 1985 squall-line system. These sections were chosen because they are nearly perpendicular to the convective line and, taken together, elucidate key features of the mesoscale flow pattern. As viewed in Fig. 1, the system moved from left to right at about 14 m/s. Other important aspects of this storm, including its horizontal reflectivity structure, are described by Houze and Rutledge (1986).

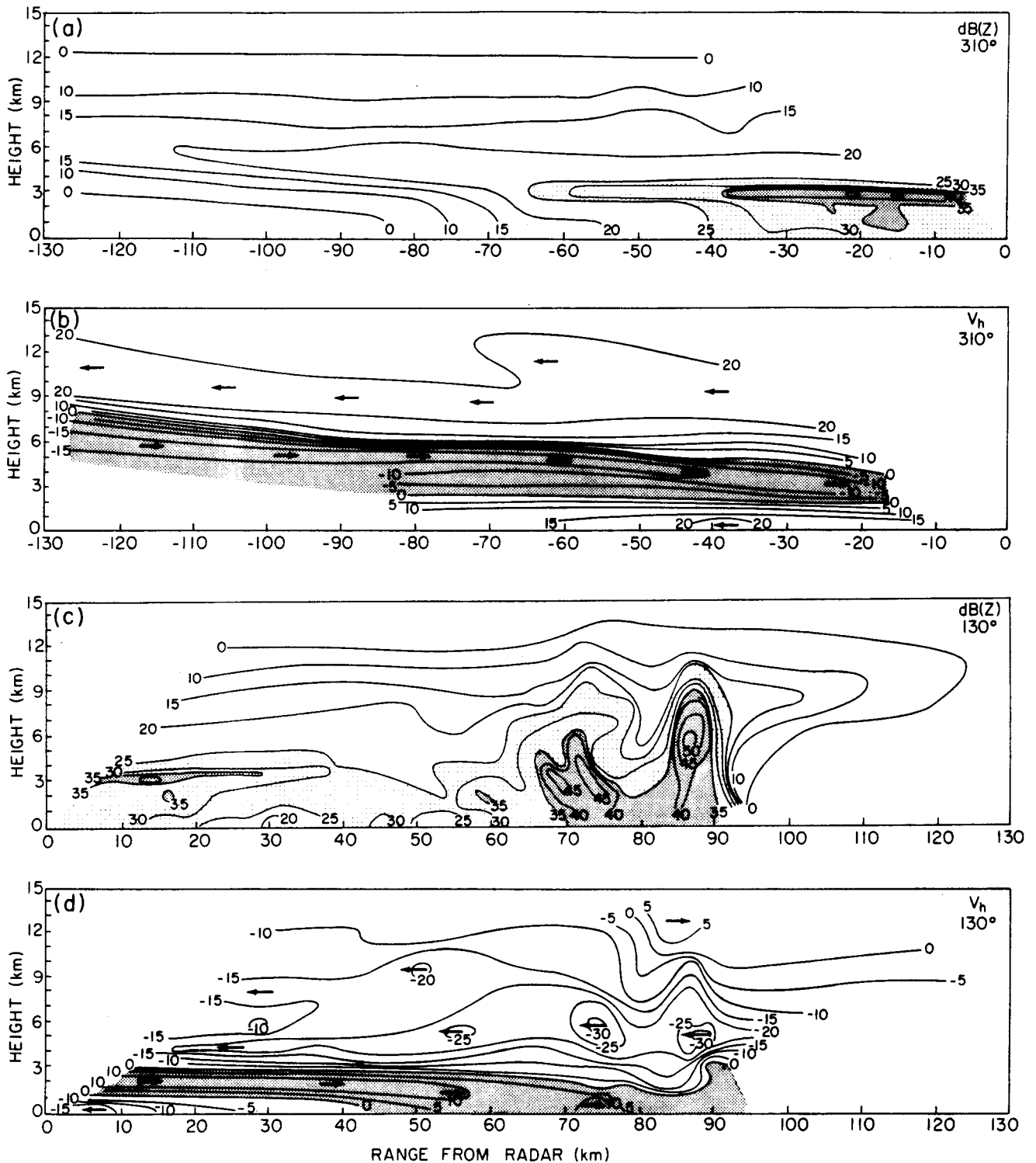


Figure 1. Vertical (range-height) cross sections reconstructed from CP-4 radar volume scan conducted at 0345-0353 GMT on 11 June 1985. Panels (a) and (b) show patterns of radar reflectivity [contour interval 5 dB(Z)] and horizontal velocity ( $V_h$ , contour interval 5 m/s) in the plane of the cross section, respectively, along 310° azimuth. Panels (c) and (d) are analogous presentations along 130° azimuth. In (a) and (c), light and dark shading highlight reflectivities in excess of 25 and 35 dB(Z). In (b) and (d), arrows indicate direction of flow, and the "rear inflow jet" feature is shaded. The 310° and 130° sections may be thought of as the left and right halves of a continuous section joined at 0 km range.

The reflectivity pattern [Figs. 1(a) and (c)] shows the leading line of convective cells (in the 50–90 km range interval) trailed by an extensive region of stratiform precipitation marked by a continuous bright band (from –65 to +40 km range) at the melting level; these contrasting regimes are separated by a narrow transition zone (Smull and Houze, 1986) characterized by a reflectivity minimum at low levels, which is evident in the 40–50 km range interval. While the region of continuous precipitation at the surface extends over 150 km, the detectable echo aloft (comprising both the leading and trailing anvil structures) exceeds 250 km in front-to-rear extent. As the volume scan was conducted, the most intense stratiform precipitation [the “secondary maximum” of reflectivity referred to by Houze and Rutledge (1986)] passed over the radar—evidenced by increased peak reflectivity values at the melting level and a deepening of the bright band echo at ranges between –20 and +20 km in Fig. 1.

The corresponding velocity analysis [Figs. 1(b) and (d)] clearly illustrates the rear inflow jet. The strongest flow approaching the system from the rear (i.e., directed from left to right in Fig. 1) slopes downward along the base of the trailing anvil echo; this juxtaposition strongly suggests that the rear inflow is associated with substantial evaporation of stratiform precipitation falling into it.

The maximum flow enters the trailing stratiform region above the melting level and continues forward and downward through the melting layer. After crossing the transition zone, it merges with outflow from convective downdrafts spreading below intense cells (e.g., the pocket of velocities in excess of 10 m/s at 75 km) and continues forward toward the leading gust front (not visible in Fig. 1). Thus, both mesoscale and convective-scale airflows appear to exert a control on the strength and propagation of the gust front, and hence the convective line itself.

Immediately above the rear inflow jet is found an opposing front-to-rear (right-to-left) relative flow maximum. This feature originates ahead of the squall line (as shown by relative speeds < –20 m/s at the 6 km level near 95 km range in Fig. 1b), but markedly deepens and strengthens as it passes through the convective zone. Local speed maxima (identified by closed –30 m/s contours near 74 and 88 km range) develop in association with convective cells. In a manner consistent with the results of Smull and Houze (1986), these speed maxima tend to appear immediately upstream (ahead) of convective reflectivity cores at middle levels, and act to reinforce the mesoscale front-to-rear flow. Laden with precipitation and cloud-ice particles from the convective cells, this current continues rearward and upward across the trailing anvil echo.

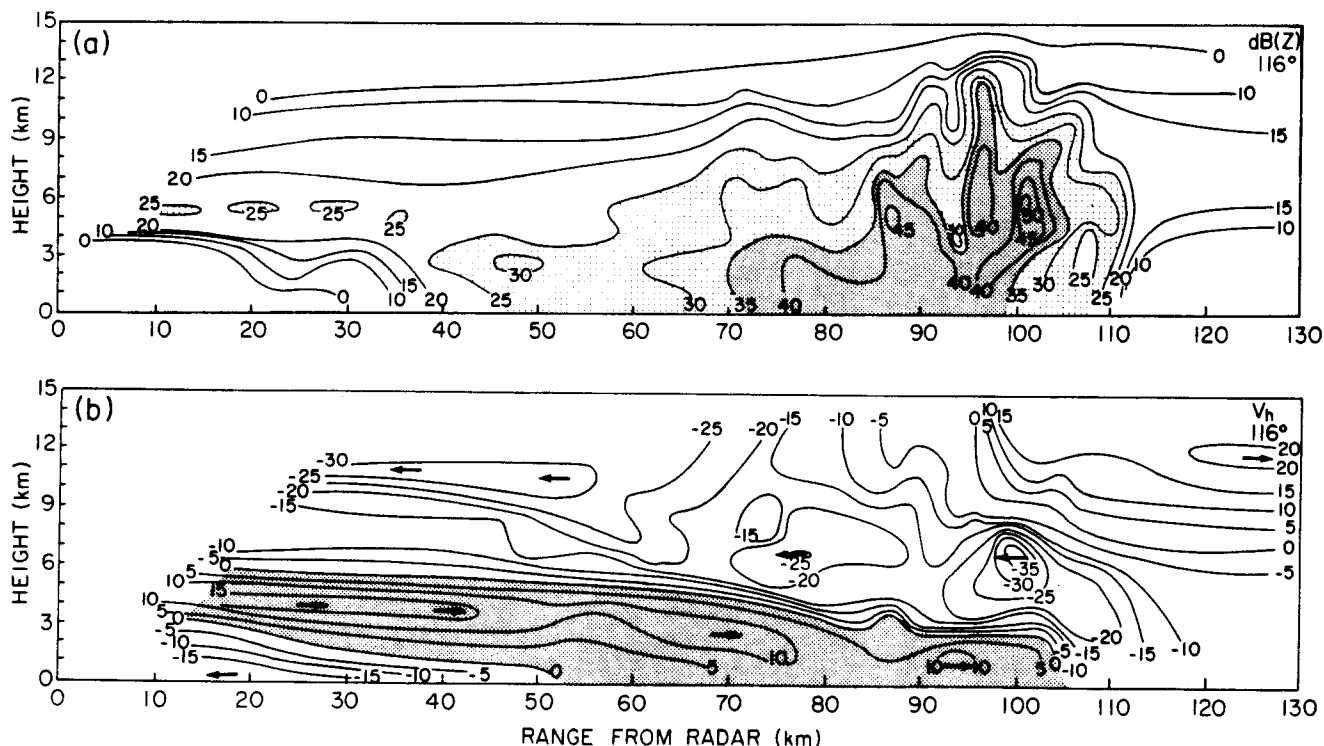


Figure 2. Vertical (range-height) cross section along 116° azimuth reconstructed from CP-4 radar volume scan conducted at 1301–1313 GMT on 28 May 1985. Panels (a) and (b) show patterns of radar reflectivity [contour interval 5 dB(Z)] and horizontal velocity ( $V_h$ , contour interval of 5 m/s) in the plane of the cross section, respectively. In (a), light and dark shading highlight reflectivities in excess of 25 and 35 dB(Z). In (b), arrows indicate direction of flow and the “rear inflow jet” feature is shaded.

Thus, the two opposing mesoscale flows meet along an interface which slopes upward toward the rear of the system. A similar boundary (again marked by a zero contour of relative flow) exists between the rear inflow jet and a layer of front-to-rear flow exiting the stratiform region at low levels. An analogous arrangement of sloping flows within the trailing anvil region of an Illinois squall line has been documented by Srivastava et al. (1986).

Another example of the rear inflow jet is provided by a cross section constructed through the 28 May 1985 mesoscale convective system (Fig. 2). The leading line of convection is again approximately perpendicular to the section, and in this case moved from left to right at about 17 m/s. The width of the precipitation region seen in Fig. 2 is appreciably less than that in Fig. 1. This difference is consistent with the greater depth of the rear inflow shown in Fig. 2, which implies increased evaporation of precipitation falling from the trailing anvil. Otherwise, the two cases are quite similar in their major aspects. The leading gust front, a feature not seen in Fig. 1, was documented on 28 May; it is found near 105 km range in Fig 2b. The merger of the mesoscale rear inflow and convective cell outflows into a unified current behind the gust front is also apparent (between  $\approx$  75 and 100 km range), as are rearward velocity perturbations occurring at midlevels in conjunction with the convective cells.

### 3. Conclusions

The radar reflectivity pattern and mesoscale circulation evident on both 11 June and 28 May 1985 strongly resemble the storm organization reported by Smull and Houze (1985, 1986) for an Oklahoma squall-line system observed in 1976. In all three cases, the reflectivity structure consists of a leading zone of deep, intense cellular echoes trailed by an extensive region of stratiform echo exhibiting a bright band at the melting level; these contrasting regimes are separated by a transition zone marked by a narrow reflectivity minimum, which is most pronounced at low levels. Moreover, in all three cases the component of air motion normal to the convective line takes on a mesoscale structure characterized by sloping layers of flow, with convective-scale speed maxima superimposed in the region of convective cells. Given these similarities in reflectivity and horizontal velocity, one can easily hypothesize that the vertical motions described by Smull and Houze (1985, 1986) were also present in the PRE-STORM cases shown here. Namely, deep and intense updrafts and downdrafts accompanying the convective cells seen at the leading edge of these systems were probably correlated with the horizontal wind speed maxima seen in the horizontal velocity cross sections (implying convective-scale momentum fluxes that reinforce the mesoscale front-to-rear and rear-to-front flows), while weaker, widespread mesoscale vertical motions (ascent in the upper portion of the trailing echo marked by front-to-rear relative flow aloft and descent in the layer of downward-sloping rear inflow jet below) likely encompassed the trailing anvil region.

The repeatability of mesoscale convective systems characterized by a rear inflow jet overridden by a middle to upper level front-to-rear mesoscale jet is indicated by the two PRE-STORM cases presented here together with the case studied by Smull and Houze (1985, 1986). Also apparently common to these cases are convective cells organized such that they modify the structure and dynamics of the mesoscale system by systematically transporting momentum vertically and hydrometeors horizontally. A unified and quantitative description of the interaction of convective-scale and mesoscale circulations and precipitation processes in mesoscale convective systems awaits further analysis of the rich PRE-STORM data set as well as future modeling studies. The repeatability of the mesoscale structure seen in these cases, however, offers a basis upon which these studies can build the desired physical and dynamical explanations.

### Acknowledgements

This research was sponsored by National Science Foundation Grants ATM-8413546 and ATM-8419543, the National Center for Atmospheric Research, and the National Oceanic and Atmospheric Administration.

### References

- Houze, R.A., Jr., and S.A. Rutledge, 1986: A squall line with trailing stratiform precipitation observed during the Oklahoma-Kansas PRE-STORM experiment. (This volume)
- Marks, F.D., Jr., and R.A. Houze, Jr., 1986: Inner core structure of Hurricane Alicia from airborne Doppler radar observations. J. Atmos. Sci., (Submitted for publication).
- Smull, B.F., and R.A. Houze, Jr., 1985: A midlatitude squall line with a trailing region of stratiform rain: Radar and satellite observations. Mon. Wea. Rev., **113**, 117-133.
- Smull, B.F., and R.A. Houze, Jr., 1986: Dual-Doppler radar analysis of a mid-latitude squall line with a trailing region of stratiform rain. J. Atmos. Sci., (Submitted for publication).
- Srivastava, R. C., T. J. Matejka and T. J. Lorello, 1986: Doppler radar study of the trailing anvil region associated with a squall line. J. Atmos. Sci., **43**, 356-377.